Available online at www.sciencedirect.com
SCIENCE DIRECT®
Inorganica Chimica Acta 357 (2004) 1270–1282
Inorganica Chimica Acta
www.elsevier.com/locate/ica

Homo- and heteronuclear complexes based on arene ruthenium complexes bearing bis(diphenylphosphinomethyl)phenylphosphine (dpmp) ☆

Yasuhiro Yamamoto [a,*,1], Yuichi Sinozuka [a], Yoshihiro Tsutsumi [a], Kei Fuse [a], Katsuaki Kuge [b], Yusuke Sunada [b], Kazuyuki Tatsumi [b]

[a] *Department of Chemistry, Faculty of Science, Toho University, Miyama, Funabashi, Chiba 274-8510, Japan*
[b] *Research Center for Materials Science and Department of Chemistry, Graduate School of Science, Nagoya Uiversity, Furo-cho, Chikusa-ku, Nagoya 454-8602, Japan*

Received 21 October 2003; accepted 25 October 2003

Abstract

Reactions of $[(p\text{-cymene})RuCl_2]_2$ (**1a**) with dpmp ($(Ph_2PCH_2)_2PPh$) in the absence or presence of KPF_6 afforded the ionic complexes $[\{(p\text{-cymene})RuCl_2\}(\text{dpmp-}P^1,P^3;P^2)\{RuCl(p\text{-cymene})\}](X)$ (**2a$_1$**: X = Cl; **2a$_2$**: X = PF_6). A (*p*-cymene)RuCl moiety constructs a 6-membered ring coordinated by two terminal P atoms of the dpmp ligand and another one binds to a central P atom of the ligand. Reactions of $[(C_6Me_6)RuCl_2]_2$ (**1b**) with an excess of dpmp in the presence of KPF_6 gave a 4-membered complex $[(C_6Me_6)RuCl(\text{dpmp-}P^1,P^2)](PF_6)$ (**3b**), chelated by a terminal and a central P atom and another terminal atom is free. Use of Ag(OTf) instead of KPF_6 gave $[\{(C_6Me_6)RuCl_2(\text{dpmp})Ag\}_2](OTf)_2$ (**5b**) that the Ag atoms were coordinated by a terminal and a central P atom of each dpmp ligand. Reaction with an equivalent of dpmp in the presence of KPF_6 gave $[\{(C_6Me_6)RuCl\}(\text{dpmp-}P^1,P^2;P^3)\{(C_6Me_6)RuCl_2\}](PF_6)$ **4b**. Complex has a structure that the $(C_6Me_6)RuCl_2$ moiety coordinated to the free P atom of **3b**. Complex **3b** was treated with $MCl_2(cod)$ (M = Pd, Pt), $[Pd(MesNC)_4](PF_6)_2$ (MesNC = 2,4,6-$Me_3C_6H_2NC$) or $[Pt_2(XylNC)_6](PF_6)_2$ (XylNC = 2,6-$Me_2C_6H_3NC$), generating $[\{(C_6Me_6)RuCl(\text{dpmp})\}_2MCl_2](PF_6)_2$ (**8b**: M = Pd; **9b**: M = Pt), $[\{(C_6Me_6)RuCl(\text{dpmp})\}_2\{Pt(MesNC)_2\}](PF_6)_4$ (**10b**) and $[\{(C_6Me_6)RuCl(\text{dpmp})\}_2\{Pt_2(XylNC)_4\}](PF_6)_4$ (**11b**), respectively. Complex **3b** reacted readily with $[Cp^*MCl_2]_2$ (M = Rh, Ir) or $AuCl(SC_4H_8)$, affording the corresponding hetero-binuclear complexes $[\{(C_6Me_6)RuCl\}(\text{dpmp-}P^1,P^2;P^3)(MCl_2Cp^*](PF_6)$ (**6b**: M = Rh; **7b**: M = Ir) and $[\{(C_6Me_6)RuCl\}(\text{dpmp-}P^1,P^2;P^3)(AuCl)](PF_6)$ (**12b**). These complexes have two chiral centers. Some complexes were separated as two diastereomers by successive recrystallization. The structures of **3b**, **5b**, **6b**, **8b** and **12b** were confirmed by X-ray analyses.

Keywords: (Arene)ruthenium complex; Bis(diphenylphosphinomethyl)phenylphosphine (dpmp); Heteronuclear complex; Pentamethylcyclopentadienylrhodium (iridium); Group 11 metal

1. Introduction

The bis(diphenylphosphinomethyl)phenylphosphine (dpmp) ligand has versatile bridging and chelating coordination behaviors for bi- and mononuclear metal centers, and linear coordination mode for trinuclear metal centers. The chemistry on rhodium, iridium, gold and silver has been widely developed [1]. We have systematically explored the chemistry of palladium and platinum bearing dpmp and isocyanide ligands and the preparations of hetero-nuclear complexes based on their palladium and platinum complexes [2,3]. These complexes bearing the dpmp ligand have been essentially constructed by the square planar frameworks. The chemistry of dpmp for octahedral or quasi-octahedral complexes

☆ Supplementary data associated with this article can be found, in the online version, at doi:10.1016/j.ica.2003.10.018.

* Corresponding author. Tel.: +0668798456; fax: +0668798459.
E-mail addresses: yamamo24@sanken.osaka-u.ac.jp (Y. Yamamoto).
[1] Present address: The Institute of Scientific and Industrial Research, Osaka University. Fax: +81-52-789-2943.

0020-1693/$ - see front matter © 2003 Elsevier B.V. All rights reserved.
doi:10.1016/j.ica.2003.10.018

has attracted our attention. This configuration could be expected to lead to the formation of complexes with diverse dimensionality. Recently,s we reported that the reactions of dpmp with $[Cp^*RhCl_2]_2$ in the presence of KPF_6 gave the mononuclear or binuclear complexes, $[Cp^*RhCl(dpmp)](PF_6)$ and $[\{Cp^*RhCl_2(dpmp)RhCl_2Cp\}^*](PF_6)$ that the dpmp ligand acts as a bidentate one, depending on the reaction conditions [4,5]. Since the former complex has a free P nucleus, it can act as a precursor that led to the formation of the hetero-nuclear complexes. Use of Ag(OTf) instead of KPF_6 gave a hetero-tetranuclear complex $[\{Cp^*RhCl_2(dpmp)Ag\}_2](OTf)_2$. Our interests shifted to the ruthenium complexes that three sites of quasi-octahedral geometry were occupied by an arene ligand. We wish to describe herein the preparation of mono- and binuclear ruthenium complexes, and the transformation to the hetero tri- and tetranuclear ones based on the ruthenium complexes. Part of this paper has already been briefly reported [4].

2. Results and discussion

2.1. Preparation of mono- and binuclear complexes

The *p*-cymene complex (**1a**) was treated with dpmp in a 1:1 molar ratio, affording orange compound (**2a$_1$**) with the empirical formula of $[\{(p\text{-cymene})RuCl_2\}_2(dpmp)]$ from an elemental analysis. The molecular peak of 1084 corresponds to [molecular peak-Cl + 1]$^+$ in the FAB mass spectroscopy. The ^{1}H NMR spectrum showed two doublets at δ 0.72 and 0.87 with a 1:1 intensity ratio for methyl protons of isopropyl groups. The $^{31}P\{^1H\}$ NMR spectrum showed the presence of two kinds of phosphorus nuclei; a doublet at δ 24.1 and a triplet at δ −40.6. These results coincided with the ionic structure that a (*p*-cymene)RuCl moiety is coordinated by two terminal P atoms and another one binds to a central P atom. The ionic structure was confirmed by the fact that the NMR spectral data of $[(p\text{-cymene})RuCl(dpmp\text{-}P^1,P^3;P^2)RuCl_2(p\text{-cymene})](PF_6)$ (**2a$_2$**), generated by a similar reaction in the presence of KPF_6, are in close similarity with that of **2a$_1$**. In the UV–Vis spectra in CH_2Cl_2, the highest wavelength of **2a$_1$** appeared at λ_{max} 369 nm and that of **2a$_2$** appeared at λ_{max} ca. 380 nm. The blue shift of **2a$_1$** probably depends on stabilization of a HOMO level arising from a weak interaction between the cationic molecule and the Cl anion. An attempt to prepare a mononuclear complex was unsuccessful; the reaction with an excess of dpmp was carried out in the presence of KPF_6, generating **2a$_2$** exclusively (Scheme 1).

Hexamethylbenzene complex (**1b**) reacted readily with an excess of dpmp in the presence of KPF_6, giving two kinds of complexes (**3b(A)** and **3b(B)**) with the empirical formula of $[(C_6Me_6)RuCl(dpmp)](PF_6)$

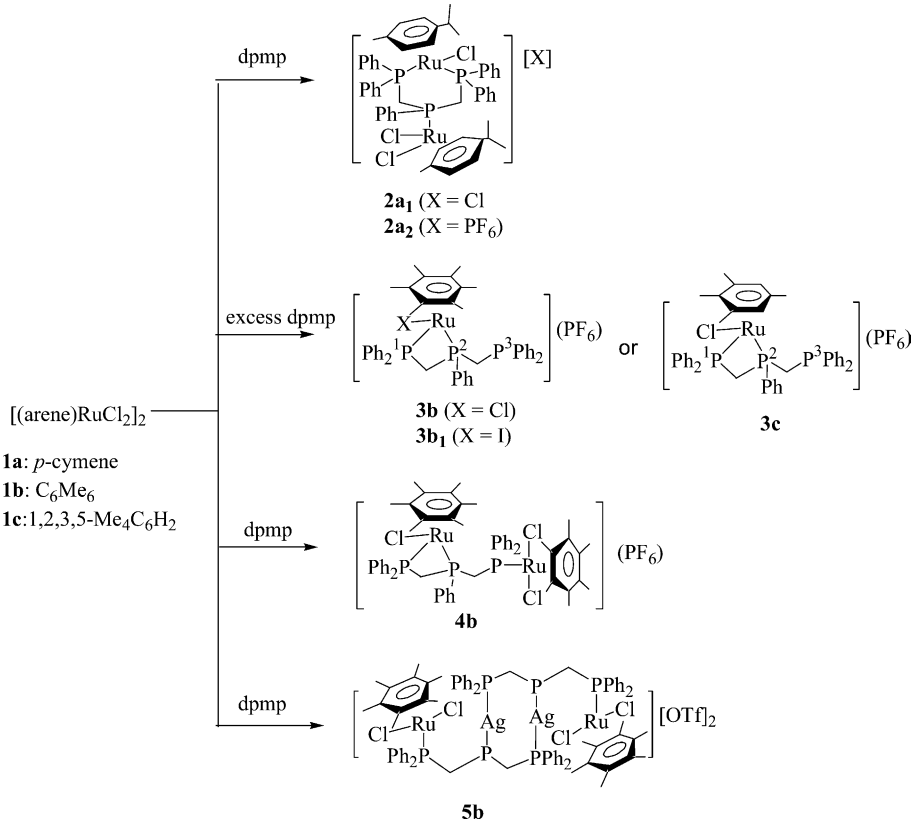

Scheme 1. Reactions of $[(arene)RuCl_2]_2$ (**1**) with dpmp in the absence or presence of KPF_6 or Ag(OTf).

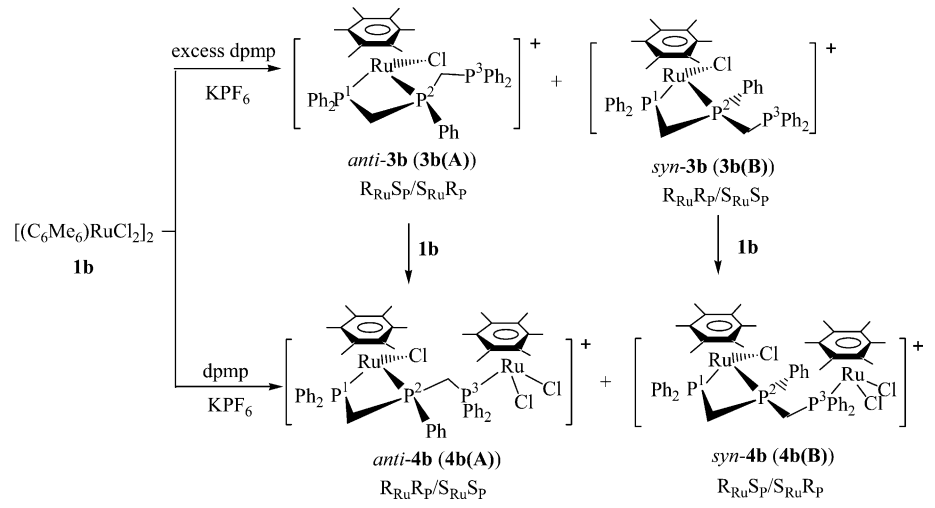

Scheme 2. Stereochemistry of mono- and binuclear complexes; the PF_6 anion was omitted for clarity.

(Scheme 2). In the ^1H NMR spectrum of the reaction mixture, the relative population of the two diastereomers was found to be 2:1 for **3b(A)** and **3b(B)**. These complexes were separated by fractional recrystallization. Iodide analogs of **3b(A)** and **3b(B)**, $[(C_6Me_6)RuI(dpmp\text{-}P^1,P^2)](PF_6)$ (**3b$_1$(A)** and **3b$_1$(B)**), were prepared by a similar reaction of $[(C_6Me_6)RuI_2]_2$ with dpmp in the presence of KPF_6. The ^1H NMR spectrum of the reaction mixture was found to be 2.5:1 for a relative population of **3b$_1$(A)** and **3b$_1$(B)**.

It was confirmed by X-ray analyses of **3b(A)** and **3b$_1$(A)** that the molecular structures consist of a 4-membered ring that the $(C_6Me_6)Ru$ moiety was coordinated by the terminal P^1 and the central P^2 atoms and a halogen atom, and another terminal P^3 atom was free (Figs. 1 and 2). These compounds have two chiral centers at the Ru and P^2 atoms. Based on the priority order of the ligands [4], both complexes are the diastereomers with a $R_{Ru}S_{P2}/S_{Ru}R_{P2}$ pair, in which we designate them as an *anti*-form (*anti*-**3b** or *anti*-**3b$_1$**), since the halogen atom sits at a *trans*-position to the P-substituted phenyl group. Thus, the other diastereomers (**3b(B)** or **3b$_1$(B)**) with a $R_{Ru}R_{P2}/S_{Ru}S_{P2}$ pair are designated as *syn*-**3b** or *syn*-**3b$_1$**.

In the separate experiments, the ^1H NMR spectra of the reaction mixtures of **3b** or **3b$_1$** were measured after 7 days, and the intensity ratios remained still constant, suggesting that the two diastereomers are not interconvertible at room temperature. Based on the formation ratio, the *anti*-form prefers to the *syn*-form.

The other arene complex such as 1,2,3,5-$Me_4C_6H_2$ (**1c**) reacted readily with an excess of dpmp in the presence of KPF_6, giving the complex (**3c**), $[(1,2,3,5\text{-}Me_4C_6H_2)RuCl(dpmp\text{-}P^1,P^2)](PF_6)$. The separation of diastereomers was not made.

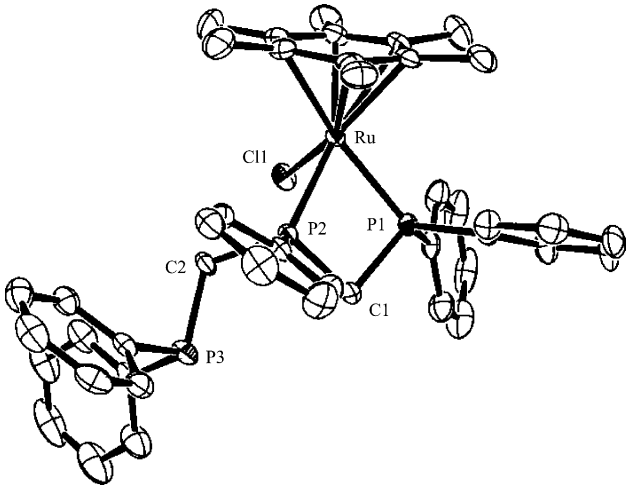

Fig. 1. Molecular structure of *anti*-**3b**; the PF_6 anion and CH_2Cl_2 were omitted for clarity.

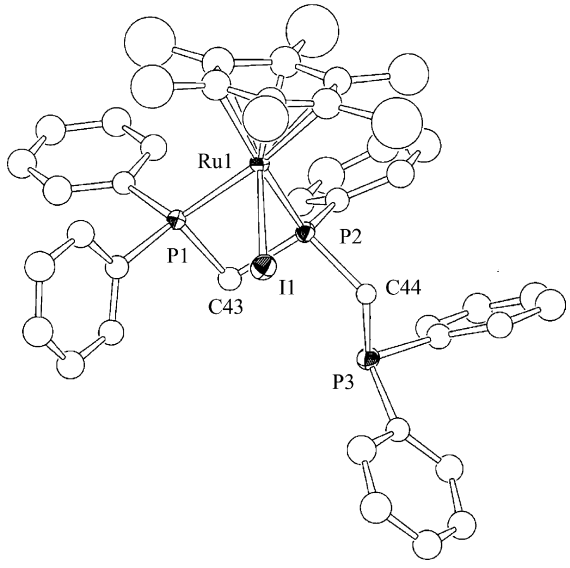

Fig. 2. Molecular structure of *anti*-**3b$_1$**; the PF_6 anion was omitted for clarity.

The reaction of **1b** with an equivalent of dpmp in the presence of KPF_6 generated two kinds of diastereomers **4b(A)** and **4b(B)**, $[(C_6Me_6)_2Ru_2Cl_3(dpmp\text{-}P^1,P^2;P^3)](PF_6)$. The ^1H NMR spectrum of the reaction mixture showed two sets of arene protons, indicating the presence of two isomers consisting of the ratio of ca. 1.3:1. Two diastereomers were separated by successive recrystallization and were not interconvertible as **3**. In the ^1H NMR spectra, the arene protons appeared at δ 1.63 and 1.97 for **4b(A)** and at δ 1.63 and 1.82 for **4b(B)**. The $^{31}P\{^1H\}$ NMR spectrum of **4b(A)** showed two doublets at δ −0.07 (d, $^2J_{P1P2} = 92.0$ Hz, P^1) and 29.3 (d, $^2J_{P3P2} = 50.0$ Hz, P^3) and a double doublet at δ −5.41 (dd, $^2J_{P2P1} = 92.0$ Hz, $^2J_{P2P3} = 50.0$ Hz, P^2), assignable to the P^1, P^3 and P^2 nucleus, respectively. In $^{31}P\{^1H\}$ NMR spectrum of **4b(B)**, two doublets due to the P^1 and P^3 nuclei appeared at δ −2.16 (d, $^2J_{P1P2} = 88.5$ Hz, P^1) and 27.1 (d, $^2J_{P3P2} = 50.0$ Hz, P^3), respectively, and a double doublet due to a P^2 nucleus appeared at δ −0.49 (dd, $^2J_{P2P1} = 88.5$ Hz, $^2J_{P2P3} = 50.0$ Hz, P^2).

In order to confirm the stereochemistry of **4b**, *anti*-**3b** was treated with **1b** in a 2:1 molar ratio, giving **4b(A)**, in comparison with the ^1H and $^{31}P\{^1H\}$ NMR spectra. Since the reaction proceeds with retention, we can assign **4b(A)** to the *anti*-form (*anti*-**4b**) with a $R_{Ru}R_P/S_{Ru}S_P$ pair and the other diastereomer (**4b(B)**) to the *syn*-form (*syn*-**4b**) with a $R_{Ru}S_P/S_{Ru}R_P$ pair on the basis of the priority order of the ligands. Thus, the stereochemistry between *anti*-**3b** and **4b(A)**, or *syn*-**3b** and **4b(B)** is similar. Analogous type of mono- and binuclear rhodium complexes has been prepared from $[Cp^*RhCl_2]_2$, dpmp and KPF_6 [4,5].

Reaction of *anti*-**4b** with xylyl isocyanide (XylNC) at room temperature led to an elimination of the Cp^*RuCl_2 fragment, generating *anti*-**3b** and $(C_6Me_6)RuCl_2$(XylNC), suggesting stability of a 4-membered ring (Scheme 3).

2.2. Preparation of heteronuclear complexes

When **1b** was treated with dpmp in a 1:2 molar ratio in the presence of Ag(OTf) instead of KPF_6, an orange complex (**5b**) formulated as a dimeric complex $[\{(C_6Me_6)RuCl_2(dpmp)Ag\}_2](OTf)_2$ was obtained, on the basis of FAB mass spectrometry. The molecular peak is *m/z* 2045, corresponding to the value of $[\{(C_6Me_6)RuCl_2(dpmp)Ag\}_2](OTf)$ (wt. 2046). The detailed structure was elucidated by X-ray analysis (Fig. 3). The complex isolated as crystals is a kind of diastereomer. A similar heteronuclear complex, $[\{Cp^*RhCl_2(dpmp)Ag\}_2](OTf)_2$, has been obtained in the reaction of $[Cp^*RhCl_2]_2$ and an excess of dpmp with Ag(OTf) [4,5].

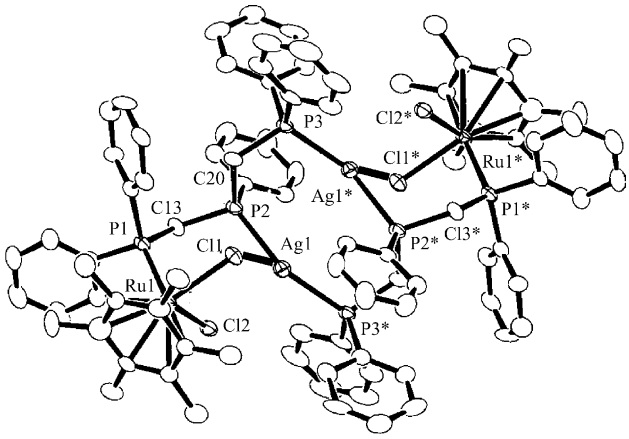

Fig. 3. Molecular structure of **5b**; the OTf anions were omitted for clarity.

Reactions of *anti*-**3b** or *syn*-**3b** with $[Cp^*RhCl_2]_2$ occurred readily, generating orange complexes formulated as $[(C_6Me_6)RuCl(dpmp\text{-}P^1,P^3;P^2)RhCl_2Cp^*](PF_6)$ (*anti*-**6b** and *syn*-**6b**) based on an elemental analysis, respectively (Scheme 4). The FAB mass spectrometry indicated the molecular peak of *m/z* 1114 for *syn*-**6b**, corresponding to the value of a cationic molecule. The crystals of *syn*-**6** were suitable for X-ray analysis. The stereochemistry of the starting complex was remained (Fig. 4). In the ^1H NMR spectra, the Cp* and arene protons appeared at δ 1.27 and 1.85 for *anti*-**6b** and at δ 1.26 and 2.02 for *syn*-**6b**, respectively. A similar reaction of *syn*-**3b** with $[Cp^*IrCl_2]_2$ also gave *syn*-**7b**, $[(C_6Me_6)RuCl(dpmp\text{-}P^1,P^3;P^2)IrCl_2Cp^*](PF_6)$, with a $R_{Ru}R_P/S_{Ru}S_P$ pair, since the reaction proceeds with retention.

In the $^{31}P\{^1H\}$ NMR spectrum of **4b**, **6b** and **7b**, the chemical shift of the P^3 nucleus bound to the Cp^*MCl_2 (M = Rh, Ir) or $(C_6Me_6)RuCl_2$ moiety appeared at δ ca. 28 for M = Rh and Ru, and at δ ca. 2 for M = Ir. A similar trend that the chemical shift of the iridium complexes appeared at a higher magnetic field than those found in the ruthenium and rhodium ones has been observed for [LMCl(BDMPP-*P*,*O*)] and [LM(TDMPP-*P*,*O*,*O*)] (LM = (arene)Ru [6], Cp*Rh [7] or Cp*Ir [8]; BDMPP-*P*,*O* = *P*Ph(2,6-$(MeO)_2C_6H_3$)

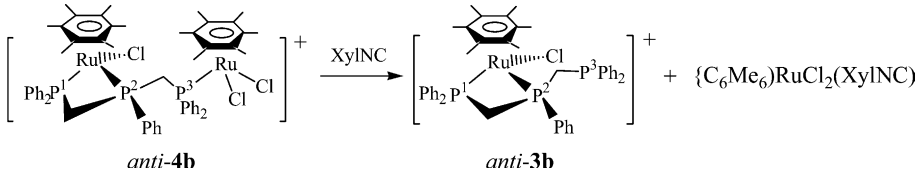

anti-**4b** *anti*-**3b**

Scheme 3. Reaction of *anti*-**4b** with xylyl isocyanide (XylNC); the PF_6 anion was omitted for clarity.

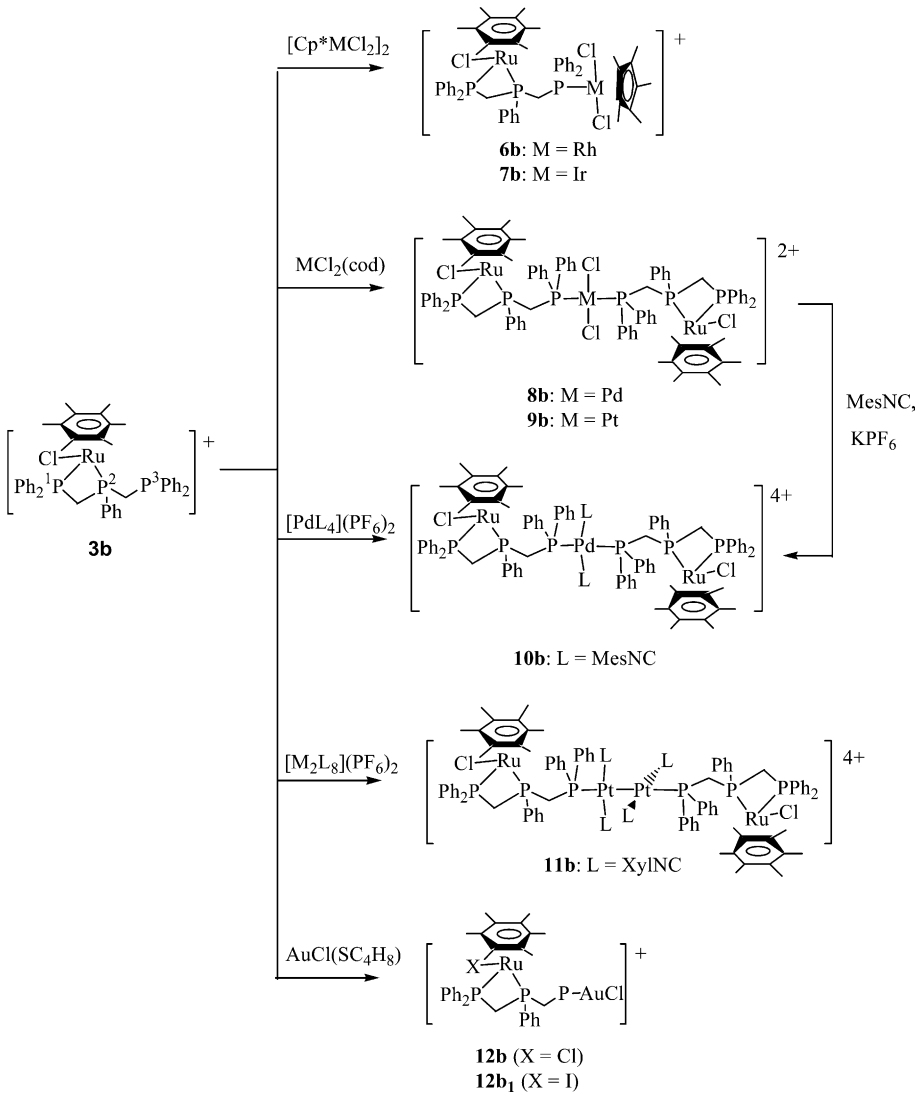

Scheme 4. Reactions of **3b** with various metal complexes; the PF_6 or OTf anions were omitted for clarity.

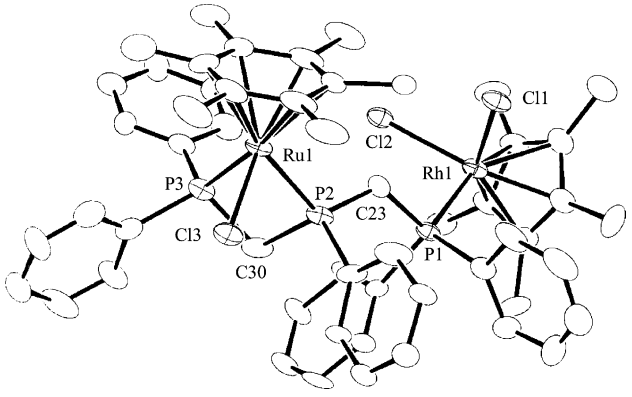

Fig. 4. Molecular structure of *syn*-**6b**; the PF_6 anion was omitted for clarity.

(2-*O*-6-$MeOC_6H_3$) or TDMPP-*P*,*O*,*O* = *P*{2,6-$(MeO)_2C_6H_3$} (2-*O*-6-$MeOC_6H_3)_2$, depending on the higher electron density on the Ir metal than for the Ru or Rh metal.

Treatment of *anti*-**3b** with $PdCl_2$(cod) or $PtCl_2$(cod) in a 2:1 molar ratio gave yellow complexes formulated as $[\{(C_6Me_6)RuCl(dpmp)\}_2MCl_2](PF_6)_2$ (**8b**: M = Pd; **9b**: M = Pt). In the ^1H NMR spectra of these complexes the arene protons appeared at δ 1.84 as a singlet, suggesting a symmetric structure. In fact the X-ray analysis of **8b** revealed that the $PdCl_2$ group binds two $(C_6Me_6)RuCl$ (dppm) moieties that are located mutually at the *trans*-positions (Fig. 5). Since the reaction proceeded stereospecifically, **9b** is also assumed to be an *anti*-form.

The $^{31}P\{^1H\}$ NMR spectrum of *anti*-**8b** indicated a singlet at δ 9.00 and two doublets at δ 5.49 and −0.86 for dpmp ligands, assignable to the P^3, P^1 and P^2 nuclei, respectively. This result showed that there are no couplings between the central P^2 atom and the terminal P^3 one, whereas in the platinum complex (*anti*-**9b**), three resonances for the P^1, P^2, and P^3 nuclei appeared at δ 2.83 ($^2J_{P1P2} = 87.7$ Hz) as a doublet, at δ 1.53 ($^2J_{P2P1} = 87.5$ Hz, $^2J_{P2P3} = 48.5$ Hz) as a double doublet

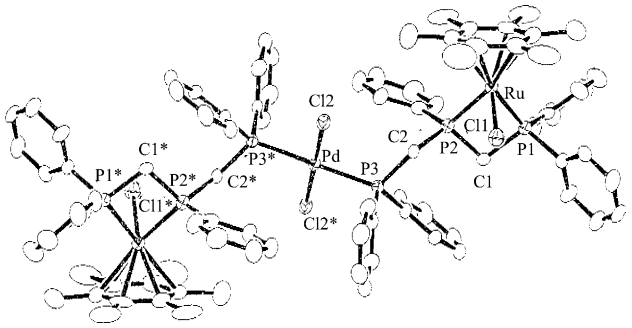

Fig. 5. Molecular structure of **8b**; the PF_6 anions were omitted for clarity.

and at δ 5.83 ($^1J_{P3Pt} = 3712$ Hz, $^2J_{P3P2} = 48.5$ Hz) as a double doublet, respectively; the latter was accompanied by satellite peaks due to ^{195}Pt nucleus.

When *anti*-**3b** was treated with $[Pd(MesNC)_4](PF_6)_2$ (MesNC = 2,4,6-$Me_3C_6H_2NC$), orange complex (**10b**) formulated as $[\{(C_6Me_6)RuCl(dpmp)\}_2\{Pd(MesNC)_2\}](PF_6)_2$ was isolated. The IR spectrum showed a sharp band at 2197 cm^{-1}, reminiscent of terminal isocyanide ligands. The ^{1}H NMR spectrum showed three characteristic singlets at δ 1.48, 1.54 and 1.87 with an intensity ratio of 1:2:3, assignable to *p*-, *m*- and arene methyl protons, respectively, suggesting a symmetric structure. The similar complex was generated by the reaction of **8b** with mesityl isocyanide in the presence of KPF_6. Reaction with a binuclear platinum complex $[Pt_2(RNC)_6](PF_6)_2$ (R = 2,6-$Me_2C_6H_3$) gave yellow crystals formulated as $[\{(C_6Me_6)RuCl(dpmp)\}_2\{Pt_2(RNC)_4\}](PF_6)_4$ (**11b**) from the elemental analysis. The atomic ratio of Pt and Ru atoms was estimated to be 1:1 from the fluorescent X-ray spectrometry. The IR spectrum showed a ν (N≡C) band at 2162 cm^{-1}. The ^{1}H NMR spectrum showed two singlets at δ 1.54 and 1.88 due to the arene and *o*-methyl protons, respectively. Since the binuclear complexes of platinum and palladium, $[M_2(RNC)_6](PF_6)_2$ (M = Pd, Pt) reacted readily with various tertiary phosphines, affording $[Pt_2(CNR)_4(PR_3)_2](PF_6)_2$ that tertiary phosphines sat at the axial positions [9], **11b** is assumed to have the molecular structure that two $(C_6Me_6)RuCl(dpmp)$ moieties occupy the axial positions of the dimeric platinum isocyanide complex.

Complexes (*anti*-**3b** and *anti*-**3b$_1$**) reacted readily with $AuCl(C_4H_8S)$, generating the corresponding complexes $[(C_6Me_6)RuX(dpmp)AuCl](PF_6)$ (*anti*-**12b**: X = Cl; *anti*-**12b$_1$**: X = I). The FAB mass spectrometry is *m*/*z* 1036 for the former and *m*/*z* 1129 for the latter, corresponding to the values of the cationic molecules. The X-ray analysis of *anti*-**12b** revealed that the reaction proceeds stereospecifically. Reaction of $[Cp^*RhCl(dpmp\text{-}P^1,P^2)](PF_6)$ with $AuCl(SC_4H_8)$ generated the tetranuclear complex, $[\{Cp^*RhCl_2(dpmp)Au\}_2](PF_6)_2$ like **5b**, whereas in the reaction with an iridium complex $[Cp^*IrCl(dpmp\text{-}P^1,P^2)](PF_6)$, a dimeric complex, $[\{Cp^*IrCl(dpmp)AuCl\}_2](PF_6)_2$ bearing an Au–Au bond has been isolated [10]. These results suggest that the reactions occur with delicate balance between the metals and ligands. There is no information on difference of reactivity at present.

2.3. Crystal structures

2.3.1. Structures of anti-3b and anti-3b$_1$

Perspective drawings with the atomic numbering scheme are given in Figs. 1 and 2, and selected bond lengths and angles are listed in Tables 1 and 2. Complex (*anti*-**3b**) contains one CH_2Cl_2 solvate molecule and has two half PF_6 moieties, one with the P atom on an inversion center and the other with the P atom on a 2-fold axis. The $(C_6Me_6)Ru$ moiety is surrounded by halogen and the terminal and central P atoms of the dpmp ligand and another terminal P atom is free. The molecular structures of both complexes are fundamentally similar to that of the rhodium complex, $[Cp^*RhCl(dpmp)](PF_6)$ [4]. The Ru-I length of 2.686(2) Å is longer by ca. 0.29 Å than that of Ru–Cl bond length and the average Ru–P length of *anti*-**3b$_1$** is longer than that of *anti*-**3b**. They are the results of great covalent radii and steric bulkiness of iodide ion. The P–Ru–P bite angles of 71.4° are compared with that of the Rh analog [4].

2.3.2. Structure of 5b

A perspective drawing with the atomic numbering scheme is given in Fig. 3, and selected bond lengths and angles are listed in Table 3. X-ray analysis revealed that the molecule has a crystallographically imposed inversion center in the middle of the Ag · Ag* vector like that of $[\{Cp^*RhCl_2(dpmp)Ag\}_2]$ [5] and each $(C_6Me_6)RuCl_2$ moiety is connected by a terminal P atom of dpmp ligands. The Ag · Cl separations (2.80–2.82 Å) are longer than those found in the Ag–Cl bridged bonds to be significant bonding between Ag and Cl atoms [11]. However, in the cubane-like cluster $[MoAg_3S_3Cl][PPh_3]_3O$ [12] and the $[Ag_2Cl_4]^{2-}$ anion in $[AsPh_4]_2[Ag_2Cl_4]$ [13], the Ag–$Cl_{bridging}$ bond lengths are in the very wide range of 2.446(2)–2.843(4) Å (2.792(4)–2.843(4) Å for the former and 2.446(2)–2.809(2) Å for the latter). Based on these results, there is likely a weak interaction between the Ag and Cl atoms. [2] The Cl(1)–Ag(1)–Cl(2) angle of 72.21(6)° is narrower by approximately 13° than that in $[\{Cp^*RhCl_2(dpmp\text{-}P,P,P)Cu\}_2](PF_6)_2$, resulting in the long Ag–Cl bond lengths in comparison with the Cu–Cl length (2.443(2) and 2.568(2) Å).

Each of two central P atoms is the chiral center. The priority order of the ligands is Ag > Ph > C^2 > C^1 for the

[2] In [5], we have reported that in the complex $[\{Cp^*RhCl_2(dpmp\text{-}P,P,P)Ag\}_2]$, the Ag···Cl separations of 2.709 and 2.911 Å is too longer to have any Ag–$Cl_{bridging}$ bond, the former length, however, is in the range of the Ag–$Cl_{bridging}$ interaction, and the Ag atoms are assumed to be three-coordinate.

Table 1
Selected bond lengths and angles for [{(C_6Me_6)RuCl}(dpmp-P^1, P^2)](PF_6) · CH_2Cl_2 (*anti*-**3b**)

Ru(1)–Cl(1)	2.4004(8)	Ru(1)–P(1)	2.3057(8)	Ru(1)–P(2)	2.3342(8)
P(1)–C(1)	1.850(3)	P(2)–C(1)	1.834(3)	P(2)–C(2)	1.835(3)
P(3)–C(2)	1.839(4)				
Cl(1)–Ru(1)–P(1)	84.33(3)	Cl(1)–Rh(1)–P(2)	83.72(3)	P(1)–Ru(1)–P(2)	71.45(3)
Ru(1)–P(1)–C(1)	96.3(1)	P(1)–C(1)–P(2)	94.7(2)	Ru(1)–P(2)–C(1)	95.8(1)
Ru(1)–P(2)–C(2)	119.2(1)	P(2)–C(2)–P(3)	112.8(2)		

Table 2
Selected bond lengths and angles for [{(C_6Me_6)RuI}(dpmp-P^1, P^2)](PF_6) (*anti*-**3b$_1$**)

Ru(1)–I(1)	2.686(2)	Ru(1)–P(1)	2.331(5)	Ru–P(2)	2.340(5)
P(1)–C(43)	1.85(2)	P(2)–C(43)	1.86(2)	P(2)–C(44)	1.82(2)
P(3)–C(44)	1.85(2)				
I(1)–Ru(1)–P(1)	84.7(1)	I(1)–Ru(1)–P(2)	85.8(1)	P(1)–Ru(1)–P(2)	71.3(2)
Ru(1)–P(1)–C(43)	96.1(6)	P(1)–C(43)–P(2)	94.4(9)	P(2)–C(44)–P(3)	111.1(9)
Ru(1)–P(2)–C(43)	95.4(6)	Ru–P(2)–C(44)	123.6(6)		

Table 3
Selected bond lengths and angles for [{(C_6Me_6)$RuCl_2$(dpmp-*P*)Ag}$_2$]($OTf)_2$ (**5b**)

Ag(1)–P(2)	2.438(2)	Ag(1)–P(3)*	2.399(3)		
Ru(1)–Cl(1)	2.428(2)	Ru(1)–Cl(2)	2.435(2)	Ru(1)–P(1)	2.356(2)
P(1)–C(13)	1.856(8)	P(2)–C(13)	1.837(9)	P(2)–C(20)	1.850(9)
P(3)–C(20)	1.850(9)				
Ag(1)–Cl(1)	2.804(3)	Ag(1)–Cl(1)	2.819(2)		
P(2)–Ag(1)–P(3)*	144.81(8)	Cl(1)–Ru(1)–Cl(2)	85.89(8)	Cl(1)–Ru(1)–P(1)	87.31(7)
Cl(2)–Ru(1)–P(1)	85.25(8)	Rh(1)–P(1)–C(13)	119.8(3)	P(1)–C(13)–P(2)	121.8(5)
Ag(1)–P(2)–C(13)	109.8(3)	Ag(1)–P(2)–C(20)	114.4(3)	P(2)–C(20)–P(3)	110.0(5)
Ag(1)*–P(3)–C(20)	113.6(3)				
Cl(1)–Ag(1)–Cl(2)	72.21(6)				

central P^2 and P^{2*}atoms, where C^1 is a methylene carbon atom between the P^1 and P^2 atoms, and C^2 atom is a methylene carbon atom between the P^2 and P^3 atoms. Complex has been identified as the $R_{P*2}S_{P2}/S_{P2}R_{P*2}$ pair. The Ag(2)P(4)C(2) eight-ring adopts a chair form. The angles around the Ru atom consisting of the P and two Cl atoms are in the range 85.3–87.3°, and are somewhat narrower than that (87.8–90.5°) in the Rh analog [5]. The P(2)–Ag–P(3)* angle of 144.81(8)° is narrower than that (149.5(2)°) for the Rh analog. The Ru–Cl and Ru–P bond lengths are longer than those found in *anti*-**3b**. The Ag(1)–P(2) length of 2.438(2) Å is longer than the Ag(1)–P(3)* length of 2.399(3) Å. They are probably responsible for release of crowdness around the Ru atoms.

2.3.3. Structure of syn-*6b*

A perspective drawing with the atomic numbering scheme is given in Fig. 4, and selected bond lengths and angles are listed in Table 4. The angles and lengths around the Ru atom are similar to those for *anti*-**3b**. The angles around the Rh atoms are near 90°. The average Rh–Cl length of 2.412 Å and the Rh–P length of 2.333 Å are compared with those in [Cp*RhCl(dpmp)$RhCl_2$ Cp*](PF_6) [4].

2.3.4. Structure of *8b*

A perspective drawing with the atomic numbering scheme is given in Fig. 5, and selected bond lengths and angles are listed in Table 5. The molecule has a crystallographically imposed inversion center on the Pd atom and each (C_6Me_6)RuCl(dpmp) moiety coordinated to a Pd atom at the *trans*-positions. The molecular structure has the four-chiral centers at two Ru atoms and two central P atoms. Stereochemistry is the *anti*-form. The bond angles and lengths around the Ru metal are similar to those found in the complexes bearing the (C_6Me_6)RuCl(dpmp) moiety. The geometry around the Pd atom is square planar. The Pd–Cl length of 2.305(2) Å and the Pd–P bond lengths of 2.351(2) Å are typical.

2.3.5. Structure of *12b*

Since the molecular structure has been briefly described in the previous communication [4], the detail is not described. The P(3)–Au–Cl(2) angle is 172.10(9)°,

Table 4
Selected bond lengths and angles for [{(C_6Me_6)RuCl}(dpmp-*P*) ($RhCl_2Cp$)](PF_6) (**6b**)

Rh(1)–Cl(1)	2.419(4)	Rh(1)–Cl(2)	2.404(5)	Rh(1)–P(1)	2.333(4)
Ru(1)–Cl(3)	2.388(4)	Ru(1)–P(2)	2.320(5)	Ru(1)–P(3)	2.314(5)
P(1)–C(23)	1.82(2)	P(2)–C(23)	1.83(2)	P(2)–C(30)	1.86(2)
P(3)–C(30)	1.85(2)				
Cl(1)–Rh(1)–Cl(2)	90.2(2)	Cl(1)–Rh(1)–P(1)	86.7(1)	Cl(2)–Rh(1)–P(1)	91.6(1)
Cl(3)–Ru(1)–P(2)	82.3(2)	Cl(3)–Ru(1)–P(3)	83.1(2)	P(2)–Ru(1)–P(3)	71.6(2)
Rh(1)–P(1)–C(23)	109.7(5)	P(1)–C(23)–P(2)	126.3(8)	Ru(1)–P(2)–C(23)	118.0(5)
P(2)–C(30)–P(3)	94.0(8)				

Table 5
Selected bond lengths and angles for [{(C_6Me_6)RuCl(dpmp-P^1,P^2)}{ $PdCl_2$}](PF_6) (**8b**)

Pd(1)–Cl(2)	2.305(2)	Pd(1)–P(3)	2.351(2)	Ru(1)–Cl(1)	2.394(2)
Ru(1)–P(1)	2.350(2)	Ru(1)–P(2)	2.316(2)	P(1)–C(1)	1.838(6)
P(1)–C(3)	1.827(7)	P(2)–C(1)	1.849(7)	P(2)–C(2)	1.834(6)
P(3)–C(2)	1.862(6)				
Cl(2)–Pd(1)–Cl(2)*	180.0	Cl(2)–Pd(1)–P(3)	88.19(6)	Cl(2)–Pd(1)–P(3)	91.81(6)
P(3)–Pd(1)–P(3)*	180.0	Pd(1)–P(3)–C(2)	116.1(2)	Cl(1)–Ru(1)–P(1)	83.26(6)
Cl(1)–Ru(1)–P(2)	84.05(6)	P(1)–Ru(1)–P(2)	71.69(6)	Ru(1)–P(1)–C(1)	94.7(2)
P(1)–C(1)–P(2)	95.6(3)	Ru(1)–P(2)–C(1)	95.5(2)	Ru(1)–P(2)–C(2)	116.6(2)
P(2)–C(2)–P(3)	121.9(3)				

near a linear array. The Au–Cl(2) and Au(1)–P(3) lengths are 2.297(2) and 2.245(2) Å, respectively. These values are compared with those found in the dimeric complex [{Cp*IrCl(dpmp)AuCl}$_2$](PF_6)$_2$ [10].

3. Experimental

3.1. General considerations

All reactions were performed under a nitrogen atmosphere. Methylene chloride was distilled from CaH_2 and diethyl ether was distilled from $LiAlH_4$. Bis(diphenylphosphinomethyl)phenylphosphine [14], [(arene)$RuCl_2$]$_2$ (arene = *p*-cymene [15], C_6Me_6[16]), [Cp*$RhCl_2$]$_2$ [17], [Cp*$IrCl_2$]$_2$ [8], AuCl(SC_4H_8) [18] and [Pt_2(XylNC)$_6$](PF_6) [20] were prepared according to the literature. The infrared and electronic absorption spectra were recorded on FT/IR-5300 and U-best 30 instruments, respectively. ^{1}H NMR spectra were measured on a JEOL EPC400 instrument at 400 MHz and ^{31}P{^{1}H} NMR spectra were measured at 161 MHz using 85% H_3PO_4 as an external reference.

3.2. Preparation of [{(p-cymene)$RuCl_2$}(dpmp-P^1,P^3;P^2)$RuCl$(p-cymene)]Cl (**2a$_1$**)

A mixture of [(*p*-cymene)$RuCl_2$]$_2$ (84.1 mg, 0.13 mmol) and dpmp (70.5 mg, 0.13 mmol) in CH_2Cl_2 (20 ml) was stirred at room temperature for 3 h. The solution was concentrated and diethyl ether was added, giving orange crystals of **2a$_1$** (123.7 mg, 79.6%). IR (nujol): 835 cm^{-1} (PF_6). UV–Vis (CH_2Cl_2): λ_{max} 369, 230(sh) nm. FAB mass: m/z 1084 ([M + 1]$^+$) (M = cationic molecule). ^{1}H NMR ($CDCl_3$): δ 0.72 (d, J_{HH} = 7.0 Hz, *Me*CH, 6H), 0.87 (d, J_{HH} = 7.0 Hz, *Me*CH, 6H), 1.71 (s, Me, 6H), 2.45 (sep., CH, J_{HH} = 7.0 Hz, 2H), 2.80 (d, $^2J_{HH}$ = 7.5 Hz, CH_2, 1H), 2.87 (d, $^2J_{HH}$ = 7.5 Hz, CH_2, 1H), 3.10 (d, $^2J_{HH}$ = 7.5 Hz, CH_2, 1H), 3.18 (d, $^2J_{HH}$ = 7.5 Hz, CH_2, 1H), 4.89 (AB system, d, $^2J_{HH}$ = 5.5 Hz, C_6H_4, 2H), 4.97 (AB system, d, $^2J_{HH}$ = 5.5 Hz, C_6H_4, 2H), 5.03 (AB system, d, $^2J_{HH}$ = 5.5 Hz, C_6H_4, 2H), 5.17 (AB system, d, $^2J_{HH}$ = 5.5 Hz, C_6H_4, 2H), 5.27 (s, CH_2Cl_2), 6.4–8.4 (c, Ph, 25H). ^{31}P{^{1}H} NMR ($CDCl_3$): δ 24.1 (d, $^2J_{PP}$ = 30.1 Hz), −40.6 (t, $^2J_{PP}$ = 30.1 Hz). *Anal*. Calcd for $C_{52}H_{57}P_3Cl_4Ru_2 \cdot 2CH_2Cl_2$: C, 50.33; H, 4.77. Found: C, 50.96; H, 4.83%.

3.3. Preparation of [{(p-cymene)$RuCl_2$}(dpmp-P^1,P^3;P^2){$RuCl$(p-cymene)}](PF_6) (**2a$_2$**)

A mixture of **1a** (102.2 mg, 0.167 mmol), dpmp (100.6 mg, 0.199 mmol) and KPF_6 (41.1 mg, 0.223 mmol) was stirred in CH_2Cl_2 (10 ml) and acetone (10 ml) at room temperature. After 12 h, the solvent was removed to dryness, the residue was washed with diethyl ether and extracted with CH_2Cl_2. The CH_2Cl_2 solution was concentrated to ca. 3 ml and diethyl ether was added, giving reddish brown compound **2a$_2$** (148.4 mg, 70.3%). IR(nujol): 837 cm^{-1} (PF_6). UV–Vis (CH_2Cl_2): λ_{max} ca. 380 nm. ^{1}H NMR ($CDCl_3$): δ0.72 (d, $^2J_{HH}$ = 7.0 Hz, *Me*CH, 6H), 0.88 (d, $^2J_{HH}$ = 7.0 Hz, *Me* CH, 6H), 1.72 (s, Me, 6H), 2.47 (sep., d, $^2J_{HH}$ = 7.0 Hz, MeC*H*, CH, 2H), 2.96 (b, CH_2, 2H), 3.23 (b, CH_2, 2H), 4.91 (AB system, d, $^2J_{HH}$ = 5.8 Hz, C_6H_4, 2H), 4.99 (AB system, d, $^2J_{HH}$ = 5.8 Hz, C_6H_4, 2H), 5.04 (d, $^2J_{HH}$ = 5.8 Hz, C_6H_4, 2H), 5.20 (d, $^2J_{HH}$ = 5.8 Hz, C_6H_4, 2H), 6.55–7.67

(c, 25H). $^{31}P\{^{1}H\}$ NMR ($CDCl_3$): δ 24.1 (d, $^{2}J_{PP} = 30.5$ Hz, terminal P), −40.6 (t, $^{2}J_{PP} = 30.5$ Hz, central P), −143.8 (sep., $^{1}J_{PF} = 707.5$ Hz, PF_6). *Anal.* Calcd. for $C_{52}H_{57}P_3Cl_3F_6Ru_2$: C, 50.84; H, 4.68. Found: C, 51.14; H, 4.73%.

3.4. Preparation of [(C$_6$Me$_6$)RuCl(dpmp-P^1,P^2)](PF$_6$) (3b)

A mixture of $[(C_6Me_6)RuCl_2]_2$(34.2 mg, 0.051 mmol), dpmp (67.0 mg, 0.132 mmol) and KPF_6 (24.1 mg, 0.132 mmol) was stirred in CH_2Cl_2 (10 ml) and acetone (10 ml) at room temperature. After 4 h, the solvent was removed and the residue was extracted with CH_2Cl_2. The solution was concentrated and diethyl ether was added, giving yellow crystals (59.2 mg, 61.1%) of **3b**. The relative population between *anti*-**3b** and *syn*-**3b** in the reaction mixture is 2:1. Two diastereomers were separated by successive recrystallization of **3b** from CH_2Cl_2 and diethyl ether. UV–Vis (CH_2Cl_2): λ_{max} 328 nm. FAB mass: m/z 804 ($[M-2]^+$), 642 ($[M–C_6Me_6\text{-}2]^+$) (M = cationic molecule). *anti*-**3b** (= **3b(A)**): ^{1}H NMR ($CDCl_3$): δ 1.93 (s, Me, 18H), 2.84 (dd, $^{2}J_{HH} = 15.0$ Hz, $^{2}J_{HP} = 6.0$ Hz, CH_2, 1H), 3.66 (dd, $^{2}J_{HH} = 15.0$ Hz, $^{2}J_{HP} = 9.5$ Hz, CH_2, 1H), 3.93 (dt, $^{2}J_{HH} = 16.0$ Hz, $^{2}J_{HP} = J_{HP} = 12.0$ Hz, CH_2, 1H), 4.42 (dt, $^{2}J_{HH} = 16.0$ Hz, $^{2}J_{HP} = {}^{2}J_{HP} = 10.0$ Hz, CH_2, 1H), 7.0–7.6 (m, Ph, 25H). $^{31}P\{^{1}H\}$ NMR ($CDCl_3$): δ 6.08 (d, $^{2}J_{P1P2} = 90.0$ Hz, P1),−2.70 (dd, $^{2}J_{P2P1} = 90.0$ Hz, $^{2}J_{P2P3} = 50.5$ Hz, P2), −24.2 (d, $^{2}J_{P3P2} = 50.5$ Hz, P3), −143.8 (sep., $^{1}J_{PF} = 707.5$ Hz, PF_6). *syn*-**3b** (= **3b(B)**): ^{1}H NMR ($CDCl_3$): δ 2.06 (s, Me, 18H), 3.00 (dd, $^{2}J_{HH} = 15.0$ Hz, $^{2}J_{HP} = 8.5$ Hz, CH_2, 1H), 3.29 (dd, $J_{HH} = 15.0$ Hz, $J_{HP} = 5.5$ Hz, CH_2, 1H), 4.23 (dt, $^{2}J_{HH} = 15.0$ Hz, $^{2}J_{HP} = {}^{2}J_{HP} = 13.0$ Hz, H), 4.99 (c, CH_2, 1H), 7.0–7.7 (m, Ph, 25H). $^{31}P\{^{1}H\}$ NMR ($CDCl_3$): δ 5.50 (d, $^{2}J_{P1P2} = 93.0$ Hz, P1),3.87 (dd, $^{2}J_{P2P1} = 93.0$ Hz, $^{2}J_{P2P3} = 45.0$ Hz, P2), −30.2 (d, $^{2}J_{P3P2} = 45.0$ Hz, P3), −143.8 (sep., $^{1}J_{PF} = 707.5$ Hz, PF_6). *Anal.* Calcd. for $C_{44}H_{47}P_4ClF_6Ru$: C, 55.61; H, 4.99; Found: C, 54.61; H, 4.97%.

3.5. Preparation of [(C$_6$Me$_6$)RuI(dpmp-P^1,P^2)](PF$_6$) (3b$_1$)

Similarly to the preparation of **3b**, brown crystals of **3b$_1$** (114.8 mg, 63.0%) were prepared by the reaction of $[(C_6Me_6)RuI_2]_2$(90.5 mg, 0.0875 mmol) with dpmp (96.5 mg, 0.191 mmol) in the presence of KPF_6 (45.3 mg, 0.246 mmol). A relative population of **3b$_1$(A)** (= *anti*-**3b$_1$**) and **3b$_1$(B)** (= *syn*-**3b$_1$**) is 2.5:1. Two diastereomers were separated by successive recrystallization from CH_2Cl_2 and diethyl ether. *anti*-**3b$_1$**. IR(nujol): 837 cm^{-1}. *anti*-**3b$_1$** (= **3b$_1$(A)**): ^{1}H NMR($CDCl_3$): δ 2.07 (s, Me, 18H), 2.97 (dd, $^{2}J_{HH} = 6.0$ Hz, $^{2}J_{HP} = 4.8$ Hz, 1H), 4.21 (dt, $^{2}J_{HH} = 16$ Hz, $^{2}J_{HP} = {}^{2}J_{HP} = 12$ Hz, CH_2, 1H), 4.73 (dt, $^{2}J_{HH} = 9.5$ Hz, $^{2}J_{HP} = {}^{2}J_{HP} = 6.0$ Hz, CH_2, 1H), 4.84 (ddd, $^{2}J_{HH} = 16$ Hz, $^{2}J_{HP} = {}^{2}J_{HP} = 10$ Hz, 1H) 7.0–7.8 (m, Ph, 25H). $^{31}P\{^{1}H\}$ NMR ($CDCl_3$): δ 0.46 (d, $^{2}J_{P1P2} = 85.0$ Hz, P1), −9.59 (dd, $^{2}J_{P2P1} = 85.0$ Hz, $J_{P2P3} = 47.5$ Hz, P^2), −22.8 (d, $^{2}J_{P3P2} = 47.5$ Hz, P^3), −143.8 (sep., $^{1}J_{PF} = 713$ Hz, PF_6). *syn*-**3b$_1$**: ^{1}H NMR($CDCl_3$): δ 2.07 (s, Me, 18H), 3.23 (dd, $^{2}J_{HH} = 6.5$ Hz, $^{2}J_{HP} = 5.0$ Hz, 1H), 3.63 (dd, $^{2}J_{HH} = 6.0$ Hz, $^{2}J_{HP} = 4.5$ Hz, CH_2, 1H), 3.92 (dt, $^{2}J_{HH} = 9.5$ Hz, $^{2}J_{HP} = {}^{2}J_{HP} = 6.0$ Hz, CH_2, 1H), 4.59 (dt, $^{2}J_{HH} = 9.5$ Hz, $^{2}J_{HP} = {}^{2}J_{HP} = 10$ Hz, CH_2, 1H), 6.8–7.8 (m, Ph, 25H). $^{31}P\{^{1}H\}$ NMR ($CDCl_3$): δ 6.13 (d, $^{2}J_{P1P2} = 43.4$ Hz, P1), −11.2 (dd, $^{2}J_{P2P1} = 43.5$ Hz, $^{2}J_{P2P3} = 87.0$ Hz, P^2), −29.8 (d, $^{2}J_{P3P2} = 43.5$ Hz, P^3), −145.6 (sep., $^{1}J_{PF} = 713$ Hz, PF_6). *Anal.* Calcd. for $C_{44}H_{47}P_4F_6$ IRu: C, 50.73; H, 4.55. Found: C, 50.28; H, 4.52%.

3.6. Preparation of [(1,2,3,5-Me$_4$C$_6$H$_2$) RuCl(dpmp-P^1,P^2)](PF$_6$) (3c)

Similarly to the preparation of **3b** except the reaction time of 2 days, brown complex (**3c**) (33.7 mg, 55%) was obtained by a mixture of $[(1,2,3,5\text{-}Me_4C_6H_2)RuCl_2]_2$ (30.3 mg, 0.0495 mmol), dpmp (29.9 mg, 0.059 mmol) and KPF_6 (13.2 mg, 0.072 mmol). IR (nujol): 839 cm^{-1} (PF_6). UV–Vis (CH_2Cl_2): λ_{max} 380 nm. FAB mass: m/z 1083 ($[M]^+$) (M = cationic part). *Anal.* Calcd. for $C_{52}H_{57}P_4Cl_3F_6Ru_2 \cdot 1/2CH_2Cl_2$: C, 49.62; H, 4.62. Found: C, 49.49; H, 4.75%. **A**: $^{31}P\{^{1}H\}$ NMR ($CDCl_3$): δ −0.02 (d, $^{2}J_{P1P2} =$ 92.7 Hz, P1),[a]−3.67 (dd, $^{2}J_{P2P1} = 97.2$ Hz, $^{2}J_{P2P3} = 51.8$ Hz, P^2),[a] 24.1 (d, $^{2}J_{P2P3} = 51.8$ Hz, P^3),[a]−145.6 (sep., $^{1}J_{PF} = 713$ Hz, PF_6). **B**: δ −0.55 ($^{2}J_{P1P2} = 102$ Hz, P1),[b]−5.14 (dd, $^{2}J_{P2P3} = 50.2$ Hz, $^{2}J_{P2P1} = 102$ Hz, P^2),[b]28.4 (d, $^{2}J_{P2P1} = 50.2$ Hz, P^3),[b]−145.6 (sep, $^{1}J_{PF} = 713$ Hz, PF_6).

3.7. Preparation of [{(C$_6$Me$_6$)RuCl}$_2$(dpmp-P^1,P^2;P^3)](PF$_6$) (4b)

Similarly to the preparation of **3b**, yellow crystals (62.2 mg, 61%) of **4b** were obtained from a mixture of **1b** (53.0 mg, 0.079 mmol), dpmp (40.5 mg, 0.080 mmol) and KPF_6 (24.9 mg, 0.135 mmol). Similarly to 3.3, each diastereomer was isolated by successive recrystallization of **4b**. The relative population of the reaction mixture: **4b(A)** : **4b(B)** = 1.3:1. IR(nujol): 841 cm^{-1} (PF_6). UV–Vis (CH_2Cl_2): λ_{max} 371, 327 nm. *Anal.* Calcd. for $C_{54}H_{61}P_4Cl_3F_6Ru_2$: C 51.14, H 5.01. Found: C 51.09, H 5.06%. *anti*-**4b** (= **4b(A)**):^{1}H NMR ($CDCl_3$): δ 1.63 (s, Me, 18H), 1.97 (s, Me, 18H), 2.68 (dt, $^{2}J_{HH} = 16.0$ Hz, $^{2}J_{HP} = {}^{2}J_{HP} = 10.5$ Hz, CH_2, 1H), 3.59 (dt, $^{2}J_{HH} = 16.0$ Hz, $^{2}J_{HP} = {}^{2}J_{HP} = 11.0$ Hz, CH_2, 1H), 3.88 (ddd, $^{2}J_{HH} = 16.0$ Hz, $^{2}J_{HP} = 6.0$ Hz, $^{2}J_{HP} = 4.0$ Hz, CH_2, 1H), 4.21 (dt, $^{2}J_{HH} = 16.0$ Hz, $^{2}J_{HP} = {}^{2}J_{HP} = 7.00$ Hz, CH_2, 1H)), 6.9–7.8 (m, Ph, 25H). $^{31}P\{^{1}H\}$ NMR

($CDCl_3$): δ 29.3 (d, $^2J_{P3P2} = 50.0$ Hz, P3),−0.07 (d, $^2J_{P1P2} = 92.0$ Hz, P1), −5.41 (dd, $^2J_{P2P1} = 92.0$ Hz, $^2J_{P2P3} = 50.0$ Hz, P2), −143.8 (sep., $^1J_{PF} = 707.5$ Hz, PF_6). *syn*-**4b** (= **4b(B)**): ^{1}H NMR ($CDCl_3$): δ 1.65 (s, Me, 18H), 1.82 (s, Me, 18H), 3.51 (m, CH_2, 1H), 3.72 (m, CH_2, 1H), 4.12 (m, CH_2, 1H), 4.79 (m, CH_2, 1H), 6.8–7.8 (c, Ph, 25H). $^{31}P\{^1H\}$ NMR ($CDCl_3$): δ 27.1 (d, $^2J_{P3P2} = 50.0$Hz, P3), −2.16 (d, $^2J_{P1P2} = 88.5$ Hz, P1), −0.49 (dd, $^2J_{P2P1} = 88.5$ Hz, $^2J_{P2P3} = 50.0$Hz, P2), −143.8 (sep., $^1J_{PF} = 707.5$ Hz, PF_6).

3.8. Preparation of [{(C_6Me_6) $RuCl_2Ag$(dpmp-P^1,P^2, P^3)}$_2$](OTf)$_2$ (**5b**)

A mixture of **1b** (51.3 mg, 0.077 mmol), dpmp (88.1 mg, 0.172 mmol) and AgOTf (52.0 mg, 0.202 mmol) was stirred in CH_2Cl_2 (10 ml) and acetone (10 ml) at room temperature. After 4 days, the solvent was removed and the residue was extracted with CH_2Cl_2. Removal of the solvent and recrystallization of the residue from CH_2Cl_2 and diethyl ether gave orange crystals (108.0 mg, 64%) of **5b**. FAB mass: *m*/*z* 2045 ($[M + OTf - 1]^+$) (M = cationic molecule). UV(CH_2Cl_2): λ_{max} 365 nm. ^{1}H NMR(CD_2Cl_2): δ 1.63 (s, Me, 36H), 2.57, 2.88, 3.33 (c, CH_2), 6.75–8.1 (m, Ph, 50H). $^{31}P\{^1H\}$ NMR (CD_2Cl_2): δ −3.0 (c, P), 0.58 (c, P), 4.0 (c, P). *Anal*. Calcd. for $C_{90}H_{94}Ag_2Cl_4F_6O_6P_6Ru_2S_2$: C, 49.37; H, 4.33. Found: C, 49.24; H, 4.32%.

3.9. Preparation of [{(C_6Me_6) RuCl}(dpmp-P^1,P^2; P^3)$RhCl_2C_p$*](PF$_6$) (**6b**)

A mixture of *syn*-**3b** (56.3 mg, 0.0592 mmol) and [Cp*$RhCl_2$]$_2$(18.4 mg, 0.0298 mmol) in CH_2Cl_2 (10 ml) and acetone (5 ml) was stirred at room temperature for 20 h. After removal of the solvent, the residue was washed with diethyl ether. The residue was recrystallized from CH_2Cl_2 and diethyl ether, giving yellow crystals of *syn*-**6b** (= **6b(B)**) (30.2 mg, 41%). IR(nujol): 641 cm^{-1} (PF_6). UV–Vis (CH_2Cl_2): λ_{max} 401 nm. FAB mass: *m*/*z* 1114 ($[M]^+$) (M = cationic molecule). ^{1}H NMR ($CDCl_3$): δ 1.26 (d, $J_{HP} = 3.5$ Hz, Cp*, 15H), 2.02 (s, Me, 18H), 2.86 (dt, $J_{HH} = 15.5$ Hz, $J_{HP} = J_{HH} = 10.5$ Hz CH_2, 1H), 3.64 (dt, $^2J_{HH} = 15.5$ Hz, $^2J_{HP} = {}^2J_{HH} = 12.5$ Hz CH_2, 1H), 4.20 (ddd, $^2J_{HH} = 16.5$ Hz, $^2J_{HP} = 6.5$ Hz, $^2J_{HP} = 3.8$ Hz CH_2, 1H), 4.44 (dt, $^2J_{HH} = 16.5$ Hz, $^2J_{HP} = {}^2J_{HH} = 8.8$ Hz, $^2J_{HH} = 5.3$ Hz CH_2, 1H), 5.27 (s, CH_2Cl_2), 7.0–7.75 (m, Ph, 25H). $^{31}P\{^1H\}$ NMR ($CDCl_3$): δ 29.3 (dd, $^2J_{P3Rh} = 137.5$ Hz, $^2J_{P3P2} = 50.5$ Hz, P3), 4.04 (dd, $^2J_{P2P1} = 94.5$ Hz, $^2J_{P2P3} = 50.5$ Hz, P2), 0.24 (d, $^2J_{P1P2} = 94.5$ Hz, P1), −143.8 (sep., $^1J_{PF} = 711.5$ Hz). *Anal*. Calcd. for $C_{52}H_{62}Cl_4F_6P_3RhRu \cdot 1/2CH_2Cl_2$: C, 50.28; H, 4.8. Found: C, 50.64; H, 4.97%. Similarly to the preparation of **6b(B)**, *anti*-**6b** (= **6b(A)**) (55%) was obtained from *anti*-**3b** and [Cp*$RhCl_2$]$_2$. ^{1}H NMR ($CDCl_3$): δ 1.27 (d, $^1J_{HP} = 3.5$ Hz, Cp*, 15H), 1.85 (s, Me, 18H), 3.76 (m, CH_2, 1H), 4.16 (m, CH_2, 2H), 5.0 (dt, $^2J_{HH} = 16.5$ Hz, $^2J_{HP} = {}^2J_{HP} = 7.0$ Hz CH_2, 1H), 7.0–8.2 (m, Ph, 25H). $^{31}P\{^1H\}$ NMR ($CDCl_3$): δ 27.3 (dd, $^2J_{P3Rh} = 142.7$ Hz, $^2J_{P3P2} = 53.5$ Hz, P3), 3.28 (d, $^2J_{P1P2} = 91.0$ Hz, P1), −0.62 (dd, $^2J_{P2P1} = 91.0$ Hz, $^2J_{P2P3} = 53.5$ Hz, P2), −143.8 (sep., $^1J_{PF} = 711.5$ Hz, PF_6).

3.10. Preparation of [{(C_6Me_6) RuCl(dpmp-P^1,P^2; P^3)$IrCl_2Cp$}](PF$_6$)$_2$ (*syn*-**7b** = **7b(B)**)

Similarly to the preparation of (**6b**), yellow complex (46.7 mg, %) was prepared from *syn*-**3b** (49.3 mg, 0.052 mmol) and [Cp*$IrCl_2$]$_2$ (21.1 mg, 0.027 mmol). IR(nujol): 837 cm^{-1}. UV–Vis (CH_2Cl_2): λ_{max} 333 nm. FAB mass: *m*/*z* 1222 ($[M + 1]^+$) (M = cationic molecule).^{1}H NMR($CDCl_3$): δ 1.26 (d, $J_{HP} = 2.0$ Hz, Cp*, 15H), 2.03 (s, Me, 18H), 2.85 (dt, $^2J_{HH} = 16.0$ Hz, $J_{HP} = 10.8$ Hz, CH_2, 1H), 3.66 (dt, $^2J_{HH} = 16.0$ Hz, $^2J_{HP} = 12.0$ Hz, CH_2, 1H), 4.31 (ddd, $^2J_{HH} = 16.0$ Hz, $^2J_{HP} = 7.5$ Hz, $^2J_{HP} = 4.5$ Hz, CH_2, H), 4.50 (ddd, $^2J_{HH} = 16.0$ Hz, $^2J_{HP} = 10.0$ Hz, $^2J_{HP} = 6.0$ Hz, CH_2, 1H), 5.27 (s, CH_2Cl_2), 6.9–7.7 (m, Ph, 25H). $^{31}P\{^1H\}$ NMR ($CDCl_3$): δ 2.01 (d, $^2J_{P3P2} = 49.5$ Hz, P^3), 0.32 (d, $^2J_{P1P2} = 93.0$ Hz, P^1), −5.81 (dd, $^2J_{P2P3} = 93.0$ Hz, $^2J_{P2P3} = 49.5$ Hz, P^2), −143.8 (sep., $^1J_{PF} = 711.4$ Hz, PF_6). *Anal*. Calcd. for $C_{54}H_{62}Cl_3F_6IrP_4Ru \cdot 1/2CH_2Cl_2$: C, 47.06; H, 4.56. Found: C, 46.59; H, 4.55%.

3.11. Preparation of [{(C_6Me_6) Ru(dpmp-P^1,P^2; P^3)}$_2$($PdCl_2$)](PF$_6$)$_2$ (**8b**)

A mixture of *anti*-**3b** (31.0 mg, 0.033 mmol) and $PdCl_2$(cod) (5.8 mg, 0.020 mmol) was stirred in CH_2Cl_2 (15 ml) at room temperature. After 10h, the solvent was concentrated to ca. 3 ml and diethyl ether was added to form yellow crystals (32.4 mg, 94.5%). IR(nujol): 839 cm^{-1} (PF_6). UV(CH_2Cl_2): λ_{max} 348 nm. FAB mass: *m*/*z* 804 ($[M–PdCl_2\text{-}2]^+$), 642 ($[M–PdCl_2–C_6Me_6\text{-}2]^+$) (M = cationic molecule). ^{1}H NMR- ($CDCl_3$): δ 1.84 (s, Me, 36H), 3.30 (dt, $^2J_{HH} = 16$ Hz, $^2J_{HP} = {}^2J_{HP} = 10$ Hz, H), 3.58 d(t, $^2J_{HH} = 16$ Hz, $^2J_{HP} = {}^2J_{HP} = 112.4$ Hz, CH_2, H), 3.58 (c, CH_2, H), 4.59 (c, CH_2, H), 6.8–7.8 (m, Ph, 50H). $^{31}P\{^1H\}$ NMR ($CDCl_3$): δ 9.00 (s, P^3), 5.49 (d, $^2J_{P1P2} = 83.2$ Hz, P^1), −0.86 (d, $^2J_{P1P2} = 83.2$ Hz, P^2), −144.1 (sep., $^1J_{PF} = 704$ Hz, PF_6). *Anal*. Calcd. for $C_{88}H_{94}Cl_4$- $F_{12}P_8PdRu_2$: C, 50.57; H, 4.80. Found: C, 50.87; H, 4.56%.

3.12. Preparation of [{(C_6Me_6) RuCl(dpmp-P^1,P^2; P^3)}$_2PtCl_2$](PF$_6$)$_2$ (**9b**)

Similarly to the preparation of **8b**, orange complex (17.3 mg, 39%) was prepared from [{(C_6Me_6)RuCl (dpmp)}](PF$_6$) (39.4 mg, 0.042 mmol) and $PtCl_2$(cod) (9.5 mg, 0.025 mmol) in CH_2Cl_2 (15 ml) for 20h. IR(nujol): 839 (PF_6) cm^{-1}. UV(CH_2Cl_2): λ_{max} 330 nm. ^{1}H NMR

(CD_2Cl_2): δ 1.84 (s, Me, 36H), 2.64, 3.70, 4.24 (c, CH_2), 6.65–7.6 (m, Ph, 50H). $^{31}P\{^1H\}$ NMR (CD_2Cl_2): δ 5.81 (dt, $^1J_{PPt} = 3712$ Hz, $^2J_{P3P2} = 48.5$ Hz, P^3), 2.83 (d, $^2J_{P1P2} = 87.5$ Hz, P^1), 1.53 (dd, $^2J_{P2P1} = 87.5$ Hz, $^2J_{P2P3} = 48.5$ Hz, P^2), −143.8 (sep, $^1J_{PF} = 708$ Hz, PF_6). *Anal*. Calcd. for $C_{88}H_{94}Cl_4F_{12}P_8PtRu_2$: C, 48.79; H, 4.34. Found: C, 48.15; H, 4.69%.

3.13. Preparation of [{(C_6Me_6) Ru(dpmp-P^1,P^2;P^3)}$_2${Pd($MesNC)_2$}]($PF_6)_2$ (**10b**)

A mixture of *anti*-**3b** (33.5 mg, 0.0353 mmol), $PdCl_2(MesNC)_2$ (8.6 mg, 0.0184 mmol) and KPF_6 was stirred in CH_2Cl_2 (10 ml) and acetone (10 ml) at room temperature for 16 h. The solvent was removed and the residue was extracted with CH_2Cl_2. After removal of the solvent, the residue was washed with diethyl ether and recrystallized from CH_2Cl_2 and diethyl ether, giving orange complex of 10b (28.8 mg, 63%). IR(nujol): 2197 (N≡C), 839 (PF_6) cm^{-1}. UV(CH_2Cl_2): λ_{max} 365 nm. ^1H NMR(CD_2Cl_2): δ 1.48 (s, 4-Me, 6H), 1.54 (s, 2-Me, 12H), 1.87 (s, arene Me, 36H), 3.4–5.4 (c, CH_2, 8H), 6.70 (s, 3-H, 4H), 7.0–7.7 (m, Ph, 50H). *Anal*. Calcd. for $C_{108}H_{116}Cl_2F_{24}N_2P_{10}PdRu_2$: C, 50.14; H, 4.52; N, 1.08. Found: C, 50.91; H, 4.95; N, 1.08%.

3.14. Preparation of [{(C_6Me_6) RuCl(dpmp-P^1,P^2;P^3)}$_2${$Pt_2(XylNC)_4$}]($PF_6)_4$ (**11b**)

Similarly to the preparation of **10b**, orange complex **11b** (21.0 mg, 42%) was prepared by a mixture of *anti*-**3b** (30.5 mg, 0.032 mmol) and $[Pt_2(XylNC)_6](PF_6)_2$ (23.5 mg, 0.016 mmol). IR(nujol): 2162 (N≡C), 839 (PF_6) cm^{-1}. UV(CH_2Cl_2): λ_{max} 333 nm. ^1H NMR(CD_2Cl_2): δ 1.54 (s, Me, 36H), 1.88 (s, *o*-Me, 24H), 3.39 (m, CH_2, 2H), 3.93 (m, CH_2, 2H), 4.13 (m, CH_2, 2H), 4.83 (m, CH_2, 2H), 6.8–7.7 (m, Ph, 62H). Fluorescent X-ray analysis: Ru:Pt:Cl:P = 1: (1.1–1.2): 1.3–1.4): (6.0–6.2). *Anal*. Calcd. for $C_{124}H_{130}Cl_2F_{24}N_4P_{10}Pt_2Ru_2 \cdot 1/2CH_2Cl_2$: C, 47.50; H, 4.19; N, 1.78. Found: C, 47.35; H, 4.17; N, 1.77.

3.15. Preparation of [(C_6Me_6) RuCl(dpmp-P^1,P^2;P^3)AuCl](PF_6) (*anti*-**12b** = **12b(A)**)

Similarly to the preparation of **6b** except the reaction time of 15 h, yellow crystals of *anti*-**12b** (45.8 mg, 91%) were prepared by a mixture of *anti*-**3b** (40.5 mg, 0.0426 mmol) and $AuCl(SC_4H_8)$ (18.0 mg, 0.056 mmol). FAB mass: *m*/*z* 1036 ($[M-2]^+$) (M = cationic molecule). IR(nujol): 835 (PF_6) cm^{-1}. UV(CH_2Cl_2): λ_{max} 341 nm. ^1H NMR (CD_2Cl_2): δ 1.93 (s, Me, 18H), 3.14 (ddd, $J_{HH} = 16.0$ Hz, $J_{HP} = 8.0$ Hz, $J_{HP} = 10.0$ Hz, CH_2, H), 4.21 (ddd, $^2J_{HH} = 16.0$ Hz, $^2J_{HP} = 12.0$ Hz, $^2J_{HP} = 12.0$ Hz, CH_2, H), 4.84 (dt, $^2J_{HH} = 16.0$ Hz, $^2J_{HP} = {}^2J_{HP} = 10.0$ Hz, CH_2, H), 4.57 (dt, $^2J_{HH} = 16$ Hz, $^2J_{HP} = {}^2J_{HP} = 8.0$ Hz, CH_2, H), 7.0–7.75 (m, Ph, 25H). $^{31}P\{^1H\}$ NMR (CD_2Cl_2): δ 18.3 (d, $^2J_{P1P2} = 25.0$ Hz, P^1), 6.91 (d, $^2J_{P3P2} = 87.0$ Hz, P^3), −4.97 (dd, $^2J_{P2P3} = 87.0$ Hz, $^2J_{P2P1} = 25.0$ Hz, P^2), −143.8 (sep., $^1J_{PF} = 707.5$ Hz, PF_6). *Anal*. Calcd. for $C_{44}H_{47}AuCl_2F_6P_4Ru$: C 44.68, H 4.01; Found: C 44.09, H 4.12%.

3.16. Preparation of [(C_6Me_6) RuI(dpmp-P^1,P^2;P^3)AuCl](PF_6) (*anti*-**12b$_1$** = **12b$_1$(A)**)

Similarly to the preparation of **6b**, brown complex *anti*-**12b**$_1$ (34.6 mg, 46%) was generated from *anti*-**3b$_1$** (61.0 mg, 0.0586 mmol) and $AuCl(SC_4H_8)$ (18.9 mg, 0.059 mmol). FAB mass: *m*/*z* 1129 ($[M-1]^+$) (M = cationic molecule). IR(nujol): 841 (PF_6) cm^{-1}. ^1H NMR ($CDCl_3$): δ 2.07 (s, Me, 18H), 3.44 (m, CH_2, 1H), 4.63 (m, CH_2, 1H), 4.78 (m, CH_2, 1H), 5.35 (m, CH_2, 1H), 6.9–7.7 (m, Ph, 25H). $^{31}P\{^1H\}$ NMR ($CDCl_3$): δ 21.0 (d, $J^3_PP^2 = 22.8$ Hz, P^3), 2.04 (d, $J_{P1P2} = 80.0$ Hz, P^1), −13.5 (dd, $J_{P2P1} = 80.0$ Hz, $J_{P2P3} = 22.8$ Hz, P^2), −143.8 (sep., $^1J_{PF} = 707.5$ Hz, PF_6). *Anal*. Calcd. for $C_{44}H_{47}AuCl_2F_6IP_4Ru \cdot CH_2Cl_2$: C 39.77, H 3.63; Found: C 39.55, H 3.69%.

3.17. X-ray crystallography – data collection

Cell constants of *anti*-**3b$_1$**(= **3b$_1$(A)**) were determined from 20 reflections on a Rigaku AFC5S diffractometer. Intensity measurements were measured by the 2θ–ω scan method using MoKα radiation ($\lambda = 0.71069$ Å). Throughout the data collection the intensities of the three standard reflections were measured every 200 reflections as a check of the stability of the crystals and no decay was observed. Absorption corrections were made with ψ scans. Other complexes were set on a Quantum CCD/Rigaku AFC7 diffractometer. Intensity measurements were made by using Mo Kα radiation ($\lambda = 0.71069$ Å) at −80 °C for *anti*-**3b** and at 20 °C for four other complexes under a cold nitrogen stream. Four preliminary data frames were measured at 0.5° increments of ω, in order to assess the crystal quality and preliminary unit cell parameters were calculated. The cell parameters were refined using all of the reflections measured in the range $2.8° < 2\theta < 56°$. The intensity images were measured at 0.5° intervals of ω for a duration of 20 s. The frame data were integrated using a d*TREK program package and the data sets were corrected for absorption using a REQAB program. The crystal parameters along with data collections are summarized in Table 6. Intensities were collected for Lorenz and polarization effects. Atomic scattering factors were taken from the usual tabulation of Cromer and Waber [20]. Anomalous dispersion effects were included in Fcalc [21]; the values of $\Delta f'$ and $\Delta f''$ were those, Creagh and McAuley [22]. All calculations were performed using the teXsan crystallographic software package [23].

Table 6
Crystallographic data for $[(C_6Me_6)RuCl(dpmp\text{-}P^1,P^2)](PF_6)CH_2Cl_2$ *anti*-**3b**, $[(C_6Me_6)RuI(dpmp\text{-}P^1,P^2)](PF_6)$ *anti*-**3b$_1$**, $[\{(C_6Me_6)RuCl_2(dpmp\text{-}P^1;P^2,P^3)Ag\}_2](PF_6)_2$ (**5b**), $[\{(C_6Me_6)RuCl\}(dpmp\text{-}P^1,P^2;P^3)(RhCl_2Cp)](PF_6)$ (**6b**) and $[\{(C_6Me_6)RuCl(dpmp\text{-}P^1,P^2;P^3)\}_2(PdCl_2)](PF_6)_2$ (**8b**)

Complex	*anti*-**3b**	*anti*-**3b$_1$**	**5b**	**6b**	**8b**
Formula	$C_{45}H_{49}Cl_3F_6P_4Ru$	$C_{44}H_{47}F_6IP_4Ru$	$C_{90}H_{94}Ag_2Cl_4F_6O_6P_6Ru_2S_2$	$C_{54}H_{62}Cl_3F_6P_4RhRu$	$C_{90}H_{98}Cl_8F_{12}P_8PdRu_2$
Molecular weight	1035.2	1041.72	2195.37	1259.30	2247.70
Crystal system	monoclinic	monoclinic	triclinic	monoclinic	monoclinic
Space group	$C2/c$ (number 15)	$P2_1/n$ (number 14)	$P\bar{1}$ (number 2)	$P2_1/n$ (number 14)	$P2_1/c$ (number 14)
Lattice parameters					
a	22.805(1)	12.810(4)	12.577(3)	18.388(4)	9.625(4)
b	12.2283(9)	17.930(3)	14.073(2)	9.6660(4)	18.745(4)
c	33.558(2)	19.487(2)	15.302(1)	33.884(2)	25.292(2)
α	90.0	90.0	115.526(4)	90.0	90.0
β	103.229(2)	102.33(1)	98.902(4)	97.181(3)	95.200(1)
γ	90.0	90.0	103.641(5)	90.0	90.0
V	9109(1)	4373(1)	2271.1(7)	5975(1)	4544(2)
Z	8	4	2	4	4
D_{calc} (g/cm^3)	1.509	1.582	1.605	1.400	1.643
μ(Mo Kα) (cm^{-1})	7.17	12.68	10.83	8.21	19.41
Scan rate (min^{-1})	–	16	–	–	–
$2\theta_{max}$	55.0	50.0	55.6	56.4	55.3
Number of reflections measured (unique)	13 729	7693	10 255	13 673	9562
Number of reflections observed	13 074 [I$> 2.0\sigma(I)$]	3623 [$I > 3.0\sigma(I)$]	5884 [$I > 3.0\sigma(I)$]	5688 [$I > 3.0\sigma(I)$]	6942 [$I > 2.0\sigma(I)$]
Number of variables	535	255	532	535	547
R, R_w[a]	0.072, 0.068	0.080, 0.112	0.067, 0.082	0.110, 0.147	0.081, 0.094
R_1	0.057 (10 781 reflections)	0.080 (3924 reflections)	0.067	0.110	0.081
Goodness of fit[b]	2.96	1.48	2.09	2.31	2.10

[a] $R = \sum \|F_o| - |F_c\| / \sum |F_o|$ and $R_w = [\sum w(|F_o| - |F_c|)^2 / w|F_o|^2]^{1/2} (w = 1/\sigma^2(F_o))$.
[b] GOF $= [\sum w(|F_o| - |F_c|)^2 / (N_o - N_p)]^{1/2}$.

3.18. Determination of the structure

The structures of complexes except *anti*-**3b**, *anti*-**3b$_1$** and **8b** solved by direct methods, were solved by Patterson methods (DIRDIF92 PATTY) and refined on *F* values. The positions of all non-hydrogen atoms except the C and F atoms, refined isotropically in *anti*-**3b$_1$**, were refined with anisotropic thermal parameters by using full-matrix least-squares methods. All hydrogen atoms were calculated at the ideal positions with the C–H distance of 0.97 Å.

4. Conclusion

In this paper the chemistry of dpmp has been extended from the square planar complexes to the octahedral ones. In the reactions of $[(\text{arene})RuCl_2]_2$ with dpmp, complexes bearing the *anti*-form were generated preferentially for the mono- and binuclear complexes. Based on the priority of the ligands around the chiral centers at the Ru and central P atoms, the *anti*-form of the mono-nuclear complex has a $R_{Rh}S_{P2}/S_{Rh}R_{P2}$ pair and that of binuclear complexes has a $R_{Rh}R_{P2}/S_{Rh}S_{P2}$ pair. The geometry of these diastereomers is that the Cl atom and the P^2-substituted Ph group occupy the opposite side. Steric demand between the Ph group and the Cl atom might be responsible for the stereochemistry of diastereomers. Complex (**3**) is one of various ligands bearing a metal as phosphinoferrocene derivatives and can act as a strategic precursor for the preparation of mixed multiple-nuclear metal complexes.

5. Supplementary materials

Tables listing detailed crystallographic data, atomic positional parameters, and bond lengths and angles are available from the authors upon request. CCDC: 217678, 217679, 217680, 217681, 2217682 and 202044 for *anti*-**3b**, *anti*-**3b$_1$**, **5b**, **6b**, **8b** and **12b**, respectively. Crystal data (Table 1S), selected bond lengths and angles (Table 2S), and the molecular structure for **12b** are also available as supplementary material.

Acknowledgements

We thank Professor Shigetoshi Takahashi and Dr. Fumie Takei of The Institute of Scientific and Industrial Research, Osaka University for measurements of FAB mass spectroscopy. This work was partially supported by a Grant-in Aid for Scientific Research from the ministry of Education, Science, Culture, and Sports, Japan (12640545).

References

[1] A.L. Balch, Prog. Inorg. Chem. 41 (1994) 239, and references therein.
[2] (a) T. Tanase, Y. Yamamoto, Trends Organomet. Chem. (1999) 35, and references therein;
(b) T. Tanase, M. Hamaguchi, R.A. Begum, S. Yano, Y. Yamamoto, J. Chem. Soc., Chem. Commun. (1999) 745;
(c) T. Tanase, R.A. Begum, H. Toda, Y. Yamamoto, Organometallics 20 (2001) 968.
[3] T. Tanase, Bull. Chem. Soc. Jpn. 75 (2002) 1407.
[4] Y. Kosaka, Y. Shinozuka, Y. Tsutsumi, Y. Kaburagi, Y. Yamamoto, Y. Sunada, K. Tatsumi, J. Organomet. Chem. 671 (2003) 8.
[5] Y. Yamamoto, Y. Kosaka, Y. Shinozaki, Y. Tsutsumi, Y. Kaburagi, K. Kuge, Y. Sunada, K. Tatsumi, Eur. J. Inorg. Chem, in press.
[6] Y. Yamamoto, R. Sato, F. Matsuo, C. Sudoh, T. Igoshi, Inorg. Chem. 35 (1996) 2329.
[7] (a) X.-H. Han, Y. Yamamoto, J. Organomet. Chem. 561 (1998) 157;
(b) Y. Yamamoto, X.-H. Han, K. Sugawara, J. Chem. Soc., Dalton Trans. (2002) 195.
[8] Y. Yamamoto, K. Kawasaki, S. Nishimura, J. Organomet. Chem. 587 (1999) 49.
[9] Y. Yamamoto, H. Yamazaki, Organometallics 12 (1993) 933.
[10] K. Kosaka, Y. Yamamoto, unpublished report.
[11] A.L. Balch, M. Ghedini, D.E. Oram, P.R. Reedy Jr., Inorg. Chem. 26 (1987) 1223.
[12] W. Jianhui, Z. Nianyong, D. Shaowu, W. Xintao, L. Jiaxi, Polyhedron 11 (1922) 1201.
[13] A. Houlton, S.K. Ibrahim, J.R. Dilworth, J. Silver, J. Chem. Soc., Dalton Trans. (1990) 2421.
[14] R. Appel, K. Geisler, H.F. Schöler, Chem. Ber. 112 (1979) 648.
[15] M.A. Bennett, T.-N. Huang, T.W. Matheson, A.K. Amith, Inorg. Synth. 21 (1982) 74.
[16] M.A. Bennett, T.W. Matheson, G.B. Robertson, A.K. Smith, P.A. Tucker, Inorg. Chem. 19 (1980) 1014.
[17] C. White, A. Yates, P.M. Maitlis, Inorg. Synth. 29 (1992) 228.
[18] R. Uson, A. Laguna, M. Laguna, Inorg. Synth. 26 (1989) 86.
[20] (a) Y. Yamamoto, K. Takahashi, K. Matsuda, H. Yamazaki, J. Chem. Soc., Dalton Trans. (1987) 1833;
(b) Y. Yamamoto, K. Takahashi, H. Yamazaki, Chem. Lett. (1985) 201.
[20] D.T. Cromer, J.T. Waber, International Tables for X-ray Crystallography, Kynoch, Birmingham (UK), 1974, Table 2.2A.
[21] J.A. Ibers, W.C. Hamilton, Acta Crystallogr. 17 (1964) 718.
[22] D.C. Creagh, W.J. McAulley, in: International Tables for Crystallography, vol. C, 1992, Table 4.2.6.8, pp. 219–222.
[23] TEXSAN: Crystal structure analysis package, Molecular Structure Corporation, Houston, TX, 1985 and 1992.